Cement & Concrete Composites 31 (2009) 2–11

Contents lists available at ScienceDirect

Cement & Concrete Composites

journal homepage: www.elsevier.com/locate/cemconcomp

The effect of concrete pore solution composition on the quality of passive oxide films on black steel reinforcement

P. Ghods [a], O.B. Isgor [a,*], G. McRae [b], T. Miller [a]

[a] Carleton University, Department of Civil and Environmental Engineering, Ottawa, Ontario, Canada K1S 5B6
[b] Carleton University, Department of Mechanical and Aerospace Engineering, Ottawa, Ontario, Canada K1S 5B6

ARTICLE INFO

Article history:
Received 4 June 2008
Received in revised form 23 October 2008
Accepted 28 October 2008
Available online 6 November 2008

Keywords:
Passive film
Concrete
Pore solution
Corrosion
Anodic polarization
EIS
Sulfate

ABSTRACT

The effect of concrete pore solution composition on the protective properties of the oxide films that form on black reinforcing steel has been experimentally investigated using anodic polarization and electrochemical impedance spectroscopy (EIS). The tests were conducted on oxide films grown in saturated calcium hydroxide solutions that included different representative amounts of NaOH, KOH, and $Ca(SO_4)$, which are compounds that are commonly observed in most ordinary portland cement concrete types. The results of both anodic polarization and EIS tests show that pore solution composition has an effect on the protective properties of the passive oxide films and, in particular, sulfate ions $(SO_4)^{2-}$ have been shown to have a negative influence on the film quality.

1. Introduction

The corrosion of black reinforcing steel in concrete is an electrochemical process at the concrete/steel interface in which the steel is oxidized in the concrete pore solution. This process leads to metal loss, but, within the highly alkaline environment provided by concrete, steel is covered with a protective oxide film (passive layer) so that under ideal conditions losses are typically less than 1 μm/year. Losses of this magnitude are not significant and do not raise any concerns about structural integrity. However, under less-than-ideal service conditions, the steel can depassivate and lose the protective oxide film, which can lead to higher rates of metal loss (i.e., corrosion) and concerns for the structural integrity of reinforced concrete structures. Key factors affecting the depassivation and corrosion of steel in concrete include the chloride content and the pH of the pore solution around the reinforcement, the physical and the chemical properties of concrete, the surface characteristics and the chemical composition of the steel, and the presence of mechanical stresses [1,2].

The current study focuses on how differences in the chemical compositions of pore solutions affect the quality of the protective passive oxide formed on reinforcing steel. Traditionally, electrochemical studies on reinforcing steel in simulated electrolytes have been performed in saturated calcium hydroxide solutions [3–5]. Although ordinary portland cement concrete pore solutions are saturated with calcium hydroxide, $Ca(OH)_2$, they also contain different auxiliary ions depending on the type of cement and supplementary cementing materials (e.g. fly ash, slag and silica fume) [6–8]. The major ionic species include cations such as Ca^{2+}, Na^+ and K^+ and anions such as OH^- and $(SO_4)^{2-}$: Sodium and potassium ions originate from alkali oxides, such as Na_2O and K_2O, that exist in cement; and sulfate ions can come from gypsum added during cement production, or from contaminated aggregates, or mixing water [9]. It is generally understood that the complex and variable nature of concrete pore solutions requires the use of representative electrolytes for studying reinforcement corrosion [10–14]; however, how the composition of the pore solution affects the quality of the protective oxide is not as well understood. Montemor et al. [15] used Auger electron spectroscopy (AES) and X-ray photoelectron spectroscopy (XPS) to show that the compositions of various extracted concrete pore solutions can affect the nature of the passive film. Similarly, Gui and Devine [16] investigated the passive film formed on iron in mildly alkaline aqueous solutions of sodium sulfate using Raman spectroscopy, and demonstrated that the structure and the nature of the passive films are affected by the presence of sulfate ions. These studies show that the composition of the concrete pore solution affects how the passive film on rebar is formed and degraded.

In the present study, the quality of the passive oxide films, which is a measure of the ability to protect the steel from corrosion, was related to the composition of the pore solution in

* Corresponding author. Tel.: +1 613 520 2600x2984; fax: +1 613 520 3951.
E-mail address: burkan_isgor@carleton.ca (O.B. Isgor).

0958-9465/$ - see front matter © 2008 Elsevier Ltd. All rights reserved.
doi:10.1016/j.cemconcomp.2008.10.003

which the films were grown. Anodic polarization and electrochemical impedance spectroscopy (EIS) were used to characterize the oxide films on the surface of deformed black steel rebar specimens. The tests were conducted in 10 solutions designed to encompass concentrations of Ca^{2+}, Na^{+}, K^{+} and $(SO_4)^{2-}$ determined from previous concrete solution-extraction studies [6–8,17]. To mimic in-service conditions, the tests described in this study were conducted on as-received black steel rebar specimens with mill scale, without special surface preparation. Recent studies by Mahallati and Saremi [6–8,17]. on black steel showed that pickling, sand-blasting, etc., change the protective properties of the passive layer, and Li and Sagues [19] demonstrated that chloride thresholds for black steel depassivation are affected by the surface finish. Hence, the current study uses as-received black steel rebar specimens with mill scale to relate better to the majority of reinforced concrete structures in service.

2. Experimental program

2.1. Specimen preparation

Rebar specimens were prepared from a 1-m long as-received deformed black steel rebar, measuring 10 mm in nominal diameter. The composition of the black steel used in this study is provided in Table 1. The rebar was cut into 30 mm segments and a steel wire (alloy: ER316L, diameter: 0.035 in.) was spot welded to one end of each specimen, and a plastic tube was then placed around the steel wire (see Fig. 1). The middle of each specimen was then wrapped tightly with electrical tape so that 2–3 mm was left exposed at the top and bottom. The specimens were then submerged in epoxy three times. After curing the epoxy, the electrical tape was removed. As a result, the top, bottom, and edges of the specimens were covered with epoxy, and the middle was uncovered (see Fig. 1). The average area of uncovered rebar was $7.2 \pm 0.2\ cm^2$, which is a comparatively large area for anodic polarization measurements, but in accord with the standard ASTM G5-94 [20]. The large area was chosen with regard to the results of Li and Sagues [21] that suggest larger areas provide more representative average behaviour and thus better simulate the in-service conditions of steel in concrete. Finally, the exposed surfaces of the specimens were rinsed with acetone and then with distilled water to remove any residue from the electrical tape. The specimens were stored in a desiccator until testing. In addition to the as-received rebar specimens described above, additional specimens were prepared in the same fashion, except that the deformities and the mill scale were removed, to a depth of 1 mm, and the surface polished to 600 Grit.

Table 1
Steel elemental composition (average of three spectrographic results – instrument model: OneSpark).

Element	%
C	0.26
Si	0.27
Mn	1.10
Cr	0.05
Ni	0.07
Mo	<0.01
Cu	0.21
Al	<0.005
Nb	<0.01
V	<0.005
Ti	<0.005
B	<0.0005
P	0.01
S	0.03
W	<0.01
Sn	0.02
Co	0.01
Zr	<0.01

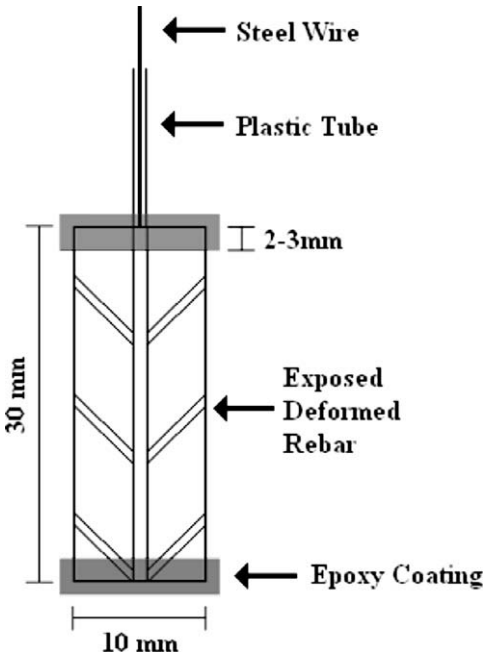

Fig. 1. An illustration of the rebar specimens.

2.2. Preparation of the synthetic pore solutions

Synthetic pore solutions were prepared from $Ca(OH)_2$, NaOH, KOH, and $CaSO_4{\cdot}2H_2O$. All solutions were saturated with $Ca(OH)_2$ to simulate conditions in ordinary portland cement concrete. Using factorial experimental design, 10 solutions were prepared with low, medium and high concentrations of the remaining three components [22]. Table 2 shows the concentrations of the chemicals added to make the solutions, as well as the ion concentration of each solution measured by inductively coupled plasma–atomic emission spectroscopy (ICP–AES) (Model: Varian Vista RL). The pH of the solutions varied between 12.3 (Solution 9) and 13.3 (Solution 4) as shown in Table 3. The conductivities of all of the solutions were high: the highest conductivity was 44.7 mS/cm for Solution 4, which had high concentrations of Na^{+} and K^{+} ions in addition to being saturated with calcium hydroxide; and the lowest was 3.74 mS/cm for Solution 10, which was saturated calcium hydroxide with no other ions added (see Table 3). The oxygen concentration of the stagnant solutions was monitored and recorded during the experiments. The results, which are presented in Table 3, indicate that the concentration of oxygen was sufficiently high in the solutions (>1 mg/L) for the oxygen reduction reaction to take place; therefore, oxygen bubbling in the solutions was not required.

2.3. Corrosion cell

Fig. 2a and b shows the cylindrical corrosion cell used to carry out both the anodic polarization and EIS tests. The 30 mm as-received black steel rebar specimen is the working electrode in the figures. The counter electrode was a co-axial platinum mesh cylindrical cage, which provided uniformly distributed electric fields around the rebar specimens. This configuration of the co-axial counter electrode allows the as-received cylindrical rebar to be

Table 2
Concentrations of the chemicals added and the ions measured in each solution using ICP–AES: the solutions were saturated with calcium hydroxide.

Solution #	Added compound (g/l)				Measured ion (M)			
	$Ca(OH)_2$	Na(OH)	K(OH)	$Ca(SO)_4 + 2H_2O$	Ca^{2+}	Na^+	K^+	$(SO_4)^{2-}$
1	Sat.	4.00	11.22	13.77	0.006	0.089	0.159	0.073
2	Sat.	8.00	22.44	27.55	0.003	0.177	0.315	0.146
3	Sat.	0.40	0.56	0.00	0.012	0.009	0.007	0.000
4	Sat.	8.00	22.44	0.00	0.000	0.170	0.306	0.000
5	Sat.	0.40	22.44	0.00	0.001	0.009	0.310	0.000
6	Sat.	0.40	22.44	27.55	0.013	0.009	0.322	0.132
7	Sat.	8.00	0.56	0.00	0.002	0.173	0.007	0.000
8	Sat.	8.00	0.56	27.55	0.011	0.180	0.007	0.065
9	Sat.	0.40	0.56	27.55	0.023	0.010	0.007	0.014
10	Sat.	0.00	0.00	0.00	0.016	0.000	0.000	0.000

Table 3
Measured values of dissolved oxygen, pH and conductivity of the synthetic pore solutions.

Solution #	Dissolved O_2 (mg/l)	pH	Conductivity mS/cm
1	3.07	12.9	17.5
2	5.28	13.2	29.8
3	6.30	12.5	4.41
4	5.38	13.3	44.7
5	3.74	13.2	32.9
6	3.73	12.8	19.3
7	5.56	12.9	17.8
8	4.47	12.6	12.0
9	6.43	12.3	4.72
10	6.35	12.4	3.74

examined over a reasonably large surface area that includes the deformity ribbing and local imperfections, as it would appear in service. A saturated calomel reference electrode (Model: Accumet) was placed in the port connected to the main body of the cell. As shown in Fig. 2a, the port includes a glass tube with a tip that was situated between the working and counter electrodes, and 5 mm away from the surface of the specimens.

2.4. Anodic polarization tests

Three replicate rebar specimens were immersed in approximately 100 ml of each synthetic pore solution; the 10 solutions containers were then sealed with parafilm in order to prevent water evaporation. For each solution, the anodic polarization experiment was carried out for each of the three rebar specimens. Anodic polarization tests were run for the first replicate specimen from each set of three in a solution (rebar 1) after five days of immersion; the second specimen (rebar 2) was tested after eight days; and the third specimen (rebar 3) was tested after at least fourteen days in each solution.

Prior to the anodic polarization experiment, the rebar specimens were removed from their solutions and then placed inside the co-axial platinum cage counter electrode (see Section 2.3). In each instance, the measurement cell was filled with the same (but filtered to remove solids) solution in which the rebar was initially immersed. The free-corrosion potential was measured with a Gamry PC4/300 Potentiostat/Galvanosatat/ZRA, relative to the saturated calomel reference electrode. It took approximately one hour before the free-corrosion potential would no longer fluctuate significantly (fluctuations were less than 1 mV/min). Subsequently,

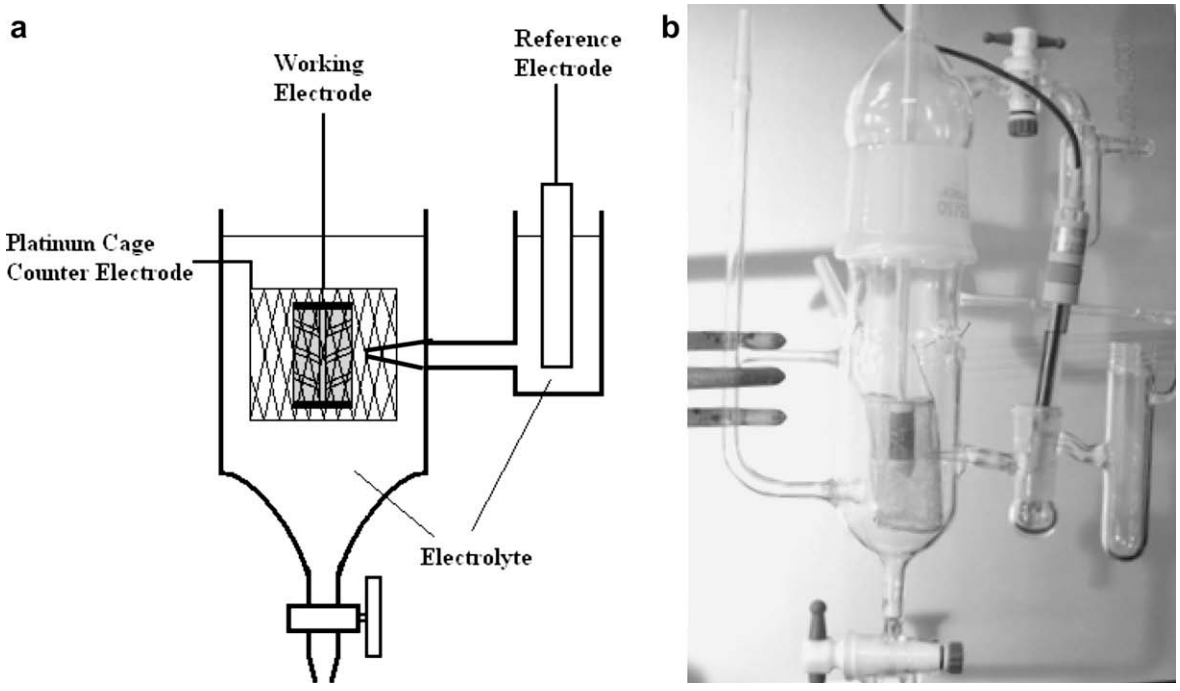

Fig. 2. (a) Schematic of the test setup used to carry out anodic polarization and EIS measurements and (b) the test setup.

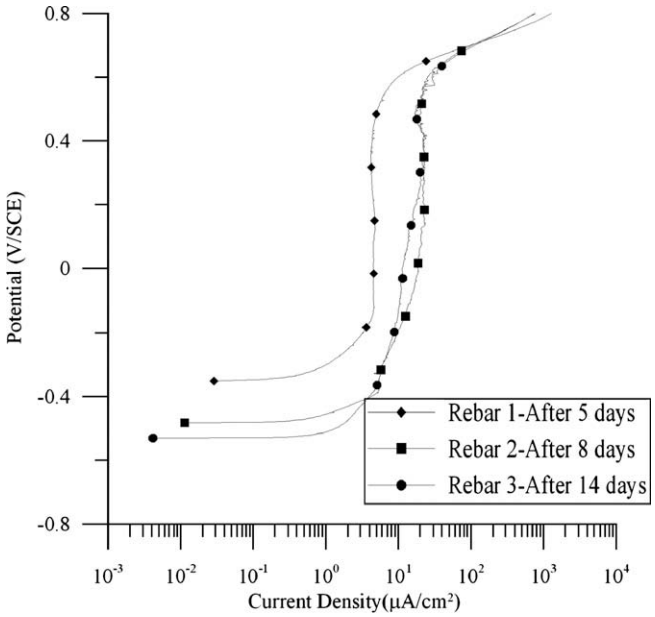

Fig. 3. Anodic polarization plots for three rebar specimens immersed in Solution 8 for different times. After eight days the polarization plots did not change significantly with further immersion; similar results were seen for rebar immersed in the other solutions.

anodic polarization curves were obtained starting 10 mV below the free potential and finishing at 800 mV SCE, using a scan rate of 0.166 mV/s, as prescribed in ASTM G5 [20]. The choice of scan rate is a compromise between accuracy and the time to complete the measurement. It was found in this study that slower scan rates did not significantly change the results, which is consistent with other studies [23–25].

The pH, dissolved oxygen, and conductivity of the solutions were measured with a VWR SympHony SP90M5. No differences in the readings were observed during immersion, or before and after each anodic polarization measurement; the results of the measurements are given in Table 3.

2.5. EIS tests

Two replicate rebar specimens were placed in covered beakers containing ~100 ml of each of the 10 synthetic pore solutions for at least 10 days, to allow the growth of stable oxide films. The rebar specimens were then placed inside the corrosion cell and EIS mea-

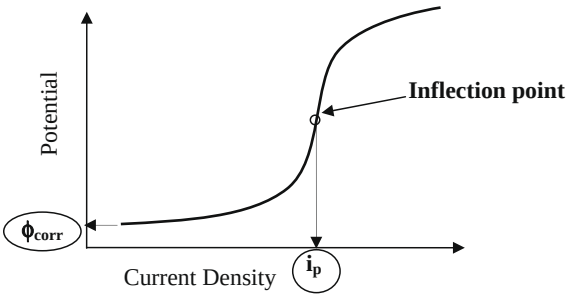

Fig. 5. Graphical definition of passive current density and free-corrosion potential used in this study.

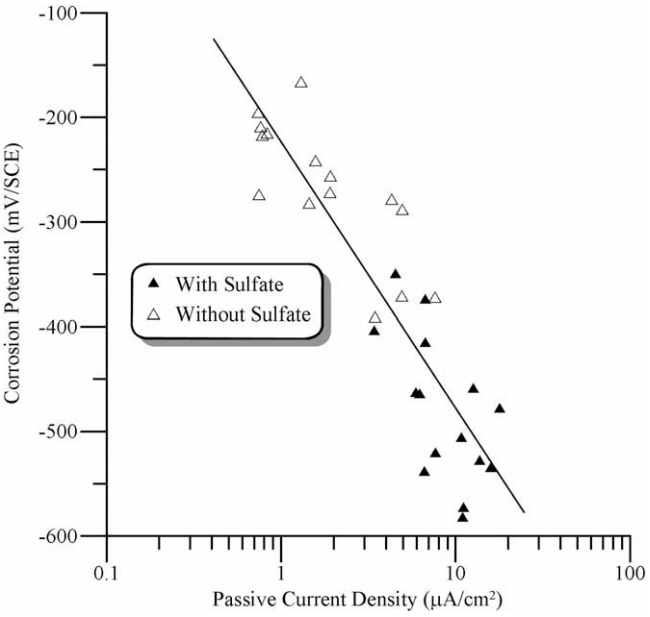

Fig. 6. The free-corrosion potential is correlated with the passive current density determined from anodic polarization tests. The line in the figure is a guide for the eye.

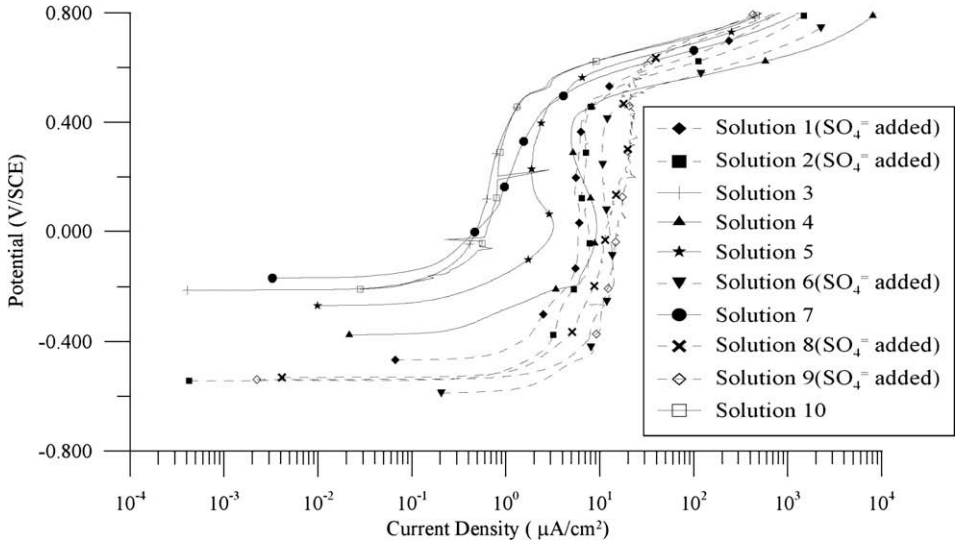

Fig. 4. The anodic polarization curves of rebar specimens that have been immersed in different synthetic pore solutions for at least 14 days, as described in the text.

surements were done in ~200 ml of the same solution, which was filtered to remove solids.

The free-corrosion potential and impedance spectrum for each rebar specimen were measured with a Gamry PC4/300 Potentiostat/Galvanosatat/ZRA, relative to the saturated calomel reference electrode. The free potentials were monitored for 2 h before EIS measurements to ensure that the oxide films had re-stabilized after transfer to the corrosion cell. The EIS measurements were done at the free potential, with an AC voltage of 10 mV RMS, between 10^5 and 10^{-3} Hz at 10 equally spaced points per decade.

No differences were observed in pH, dissolved oxygen, and conductivity of the solutions, measured with a VWR SympHony SP90M5, before and after each EIS measurement; the measurements were essentially the same as the ones reported in Table 3.

3. Results and discussion

3.1. Anodic polarization test results

Anodic polarization experiments that were carried out after 5, 8 and 14 days of immersion suggest that eight days are required for the oxides to stabilize. In Fig. 3, as an example, typical anodic polarization curves are plotted for the three sets of as-received rebar specimens immersed in solution 8 for 5, 8 and 14 days. All of the anodic polarization curves have the same general appearance; however, the curve for rebar 1, which only experienced 5 days of immersion, is shifted to lower currents compared to the curves for rebars 2 and 3, which essentially overlap. (For the second and third rebar specimens, the estimated reproducibility is ±60 mV for the free potential and ±30% for the passive current density.) The inference is that the oxide films on the rebar specimens became relatively stable after eight days of immersion in the synthetic pore solutions. Similar conclusions were drawn from observations of the free potential: large drifts of >180 mV/h during the first few hours became much smaller (<0.4 mV/h) after about eight days. These results are consistent with previous work by Poursaee and Hansson [12]. The stability of the tests after eight days of immersion indicates that reliable data can be obtained with as-received rebar.

Anodic polarization tests were also done on two specimens that had their deformities and mill scale removed and their surfaces subsequently polished. Similar polarization curves were obtained for these polished specimens; however, they were shifted to lower currents (by approximately a decade) relative to the curves for the as-received rebar specimens. These shifts are large enough to suggest that modifying the surfaces by polishing will result in conditions not representative of service. Hence, the remainder of the

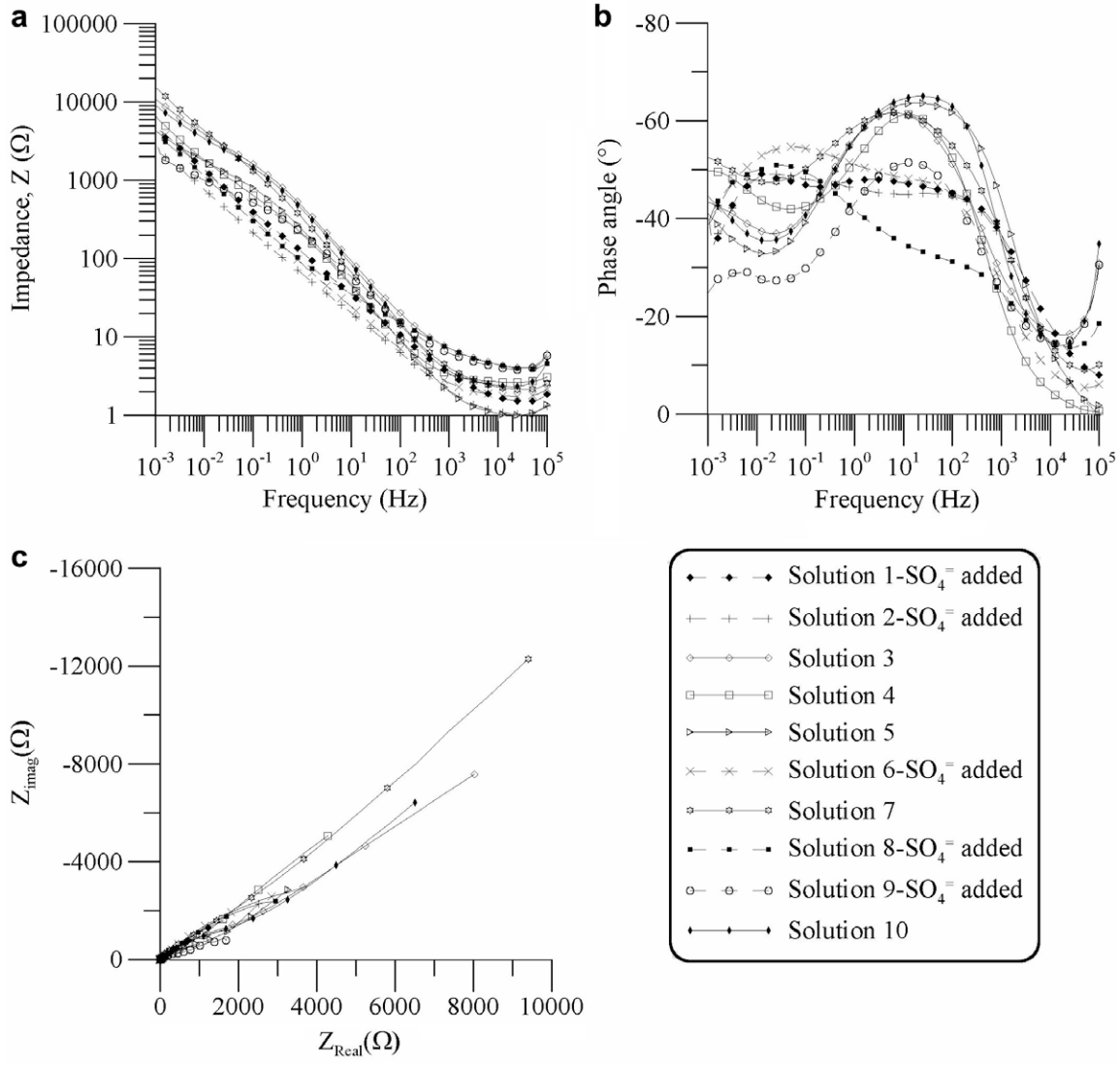

Fig. 7. Typical plots of (a) impedance vs. frequency, (b) phase angle vs. frequency and (c) imaginary vs. real impedance (Nyquist).

discussion will focus on results obtained for as-received specimens.

Anodic polarization curves obtained for as-received rebar specimens immersed for at least 14 days (i.e., rebar 3 for each solution) in the 10 simulated pore solutions are shown in Fig. 4. The large differences indicate that the characteristics of the oxide film formed in the various solutions may not be the same. For instance, consider the current density corresponding to the inflection point in the polarization plot in Fig. 5; in this paper, this current density is equated to the passive current density, i_p. Fig. 4 shows over two orders of magnitude difference in the passive current density for the different simulated pore solutions. These passive current densities are not significantly correlated with pH, conductivity or oxygen content of the solutions shown in Table 2, within the reported ranges of the values. This suggests more complicated functional dependencies, and/or that differences observed in the anodic polarization curves might originate with the oxide films that form on the rebar surface, and that the quality of the oxide layer is influenced by the pore solution in which it was grown: higher quality is characterized by lower passive current density, and vice versa. Higher passive current densities would extrapolate to higher metal loss rates and, thus these oxides would be less protective and thus of lesser quality. Fig. 4 also shows that the passive current densities for oxides grown in solutions with $(SO_4)^{2-}$ were always higher than for those grown in solutions without $(SO_4)^{2-}$.

The iron Poubaix diagram shows that for the pH range found in concrete, and in this study, iron forms a passive protective oxide as it corrodes; hence, it is reasonable to assume that all rebar specimens grown in the different synthetic pore solutions are in a passive state. A simple Evan's diagram description (plotting potential against log of the current density) of the present experiment would show all of the corrosion potentials in Fig. 4 occurring at the intersections of the cathodic line for the reduction of oxygen and the various metal oxidation lines, which would all be 'vertical' in accord with the passive state conditions. Oxides that are not as protective would passivate (become vertical on the Evan's diagram) at higher current densities and consequently the intersection of the oxygen reduction line with the passive region occurs at lower potentials, in accord with the negative Tafel slope relating the reduction overpotential to the logarithm of the current density [26]. Thus the anodic polarization curves in Fig. 4 move down (to lower corrosion potentials) and to the right (to higher current densities) as the passive films become less protective.

The present experiment provides a set of oxide films with different values for the passive current density, i_p, that can be paired with the free-corrosion potential, ϕ_{corr}, to determine the Tafel rela-

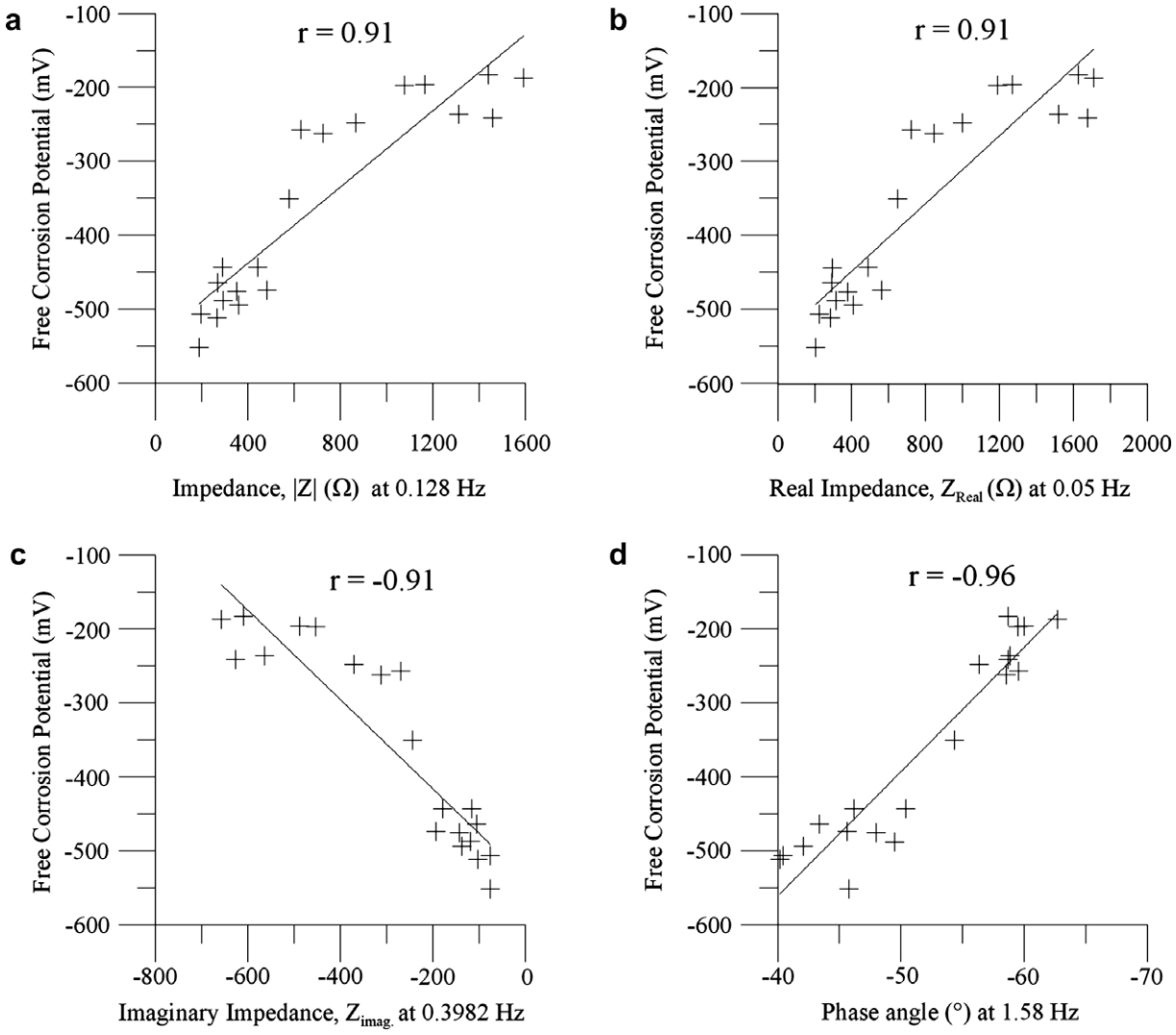

Fig. 8. Examples showing data at representative frequencies used in the calculations of the Pearson correlation coefficients shown in Fig. 9. The *r* values are 0.91, 0.91, −0.91 and −0.96 for plots (a), (b), (c) and (d), respectively.

tion for the oxygen reduction reaction on as-received black steel at high pH, because associated values of i_p and ϕ_{corr} are points on the reduction line. Fig. 6 shows the correlation between free-corrosion potential and passive current density; implicit in this plot is the pH dependence, which is small. These data can be fitted to the Tafel equation:

$$\phi_{corr} = \beta_c \log 10(i_p/i_o) + \phi_c^o \quad (1)$$

where β_c is the cathodic Tafel slope, i_o is the cathodic exchange current density, and ϕ_c^o is the equilibrium oxygen reduction potential. Assuming the oxygen reduction reaction is reversible, then [26]

$$\phi_c^o[\text{mV SCE}] = 988 - 59.2\ \text{pH} \quad (2)$$

Substituting Eq. (2) into Eq. (1) yields the regression equation used to determine the Tafel parameters from the free-corrosion potentials, passive current densities and solution pH measurements:

$$\beta_c = -245 \pm 30\ \text{mV/decade}; \quad i_o = (1.4 \pm 0.9) \times 10^{-2}\ \mu\text{A/cm}^2. \quad (3)$$

The exchange current density determined in this study is comparable to earlier experimental values [27]. The value for the determined Tafel slope is consistent with previously reported cathodic Tafel slopes for oxygen reduction in alkaline solutions and in mortars determined in the standard way from the linear region of the cathodic polarization vs. log current density plot [28–30]. The method introduced in this study for determining β_c is complementary to the standard method, which is based on cathodic polarization; however, it does not have the same difficulties with defining the extent of the linear region.

3.2. EIS test results

The anodic polarization results described in Section 3.1 suggested that the quality of the protective oxide layer may be significantly influenced by the pore solution in which it was grown. In this section, EIS is used to explore the electrochemical properties of the oxides grown in the various simulated pore solutions.

Fig. 7 shows impedance spectra plotted different ways for rebar specimens in the ten synthetic pore solutions; replicate specimens show similar results and are not plotted. Fig. 7a shows relatively large differences in the magnitude of the impedance at low frequencies (<1 Hz); these can be used to distinguish differences in the oxide film properties that form in different solutions. As an example, Fig. 7a shows the effect of adding sulfate ions. At low frequencies (<1 Hz), rebar oxides grown in $(SO_4)^{2-}$ containing solutions have lower impedance magnitudes compared with those grown in solutions without $(SO_4)^{2-}$ ions. (In the plots, the sulfate-containing

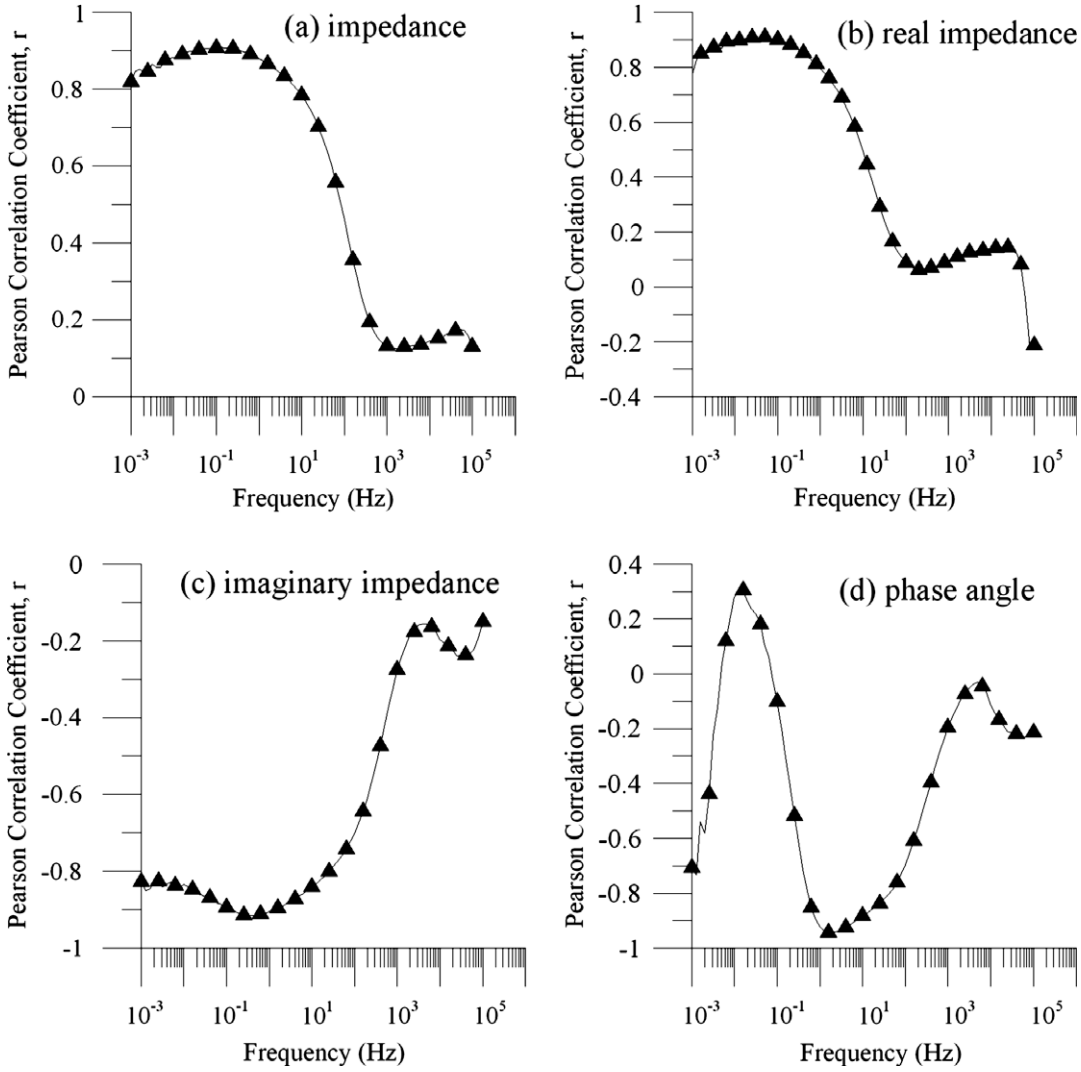

Fig. 9. Pearson correlation coefficients, r, between free-corrosion potential and (a) impedance magnitude; (b) real impedance; (c) imaginary impedance; and (d) phase angle. Correlation coefficients with $|r| > 0.45$ have p-values (i.e. the probability of an observed result happening by chance under the null hypothesis) less than 0.05.

solutions are shown as dashed lines, and the spectral points for the solutions without sulfate are connected with solid lines.) This is consistent with direct current measurements that show films with higher electrical resistances generally are more resistant to corrosion [31], and this, in turn, supports the observations made during the anodic polarization tests that the passive oxide films were less protective if they were grown in solutions containing $(SO_4)^{2-}$ ions. It can also be observed in Fig. 7b that the phase angles in different solutions show large variations. For example, in the mid-frequency region (i.e., 1–100 Hz) the phase angles of the specimens grown in solutions containing $(SO_4)^{2-}$ are generally larger than those for specimens grown in solutions without $(SO_4)^{2-}$ ions.

The observations described above can be made quantitative by calculating Pearson correlation coefficients, r, between the measured rebar free-corrosion potentials and the various EIS measures (magnitude of the impedance, real and imaginary components, and phase angle) at each measured frequency. Fig. 8 shows typical examples of plots of free-corrosion potential vs. EIS measures at specific frequencies, along with the calculated correlation coefficients. Similar correlation calculations were done at all frequencies using all the EIS measures from replicate sets of specimens in the ten synthetic pore solutions. The results are shown in Fig. 9. The free-corrosion potential tends to correlate with impedance at low frequencies, and phase angle at intermediate frequencies. The correlations with free-corrosion potential are positive and largest at approximately 0.1 Hz with the impedance magnitude, and at ≈0.05 Hz with the real component; the correlations are negative and smallest at ≈0.01 Hz with the imaginary impedance, and at ≈10 Hz with the phase angle. Because the free-corrosion potential can be related to the passive current density, as shown in the previous section, these correlations with the free-corrosion potential suggest that low-frequency impedances, and mid-frequency phase angles, can also be used in to rank the quality of the oxide films.

3.3. Discussion

Rankings of the quality of the protective oxides grown on rebar immersed in the various synthetic pore solutions are shown in Table 4. The anodic polarization experiments suggested that high quality oxides have low passive current densities and high corrosion potentials; hence the quality of the oxides can be ranked from high to low by ordering them according to low to high values of i_p, or high to low values of ϕ_{corr}. In addition, the EIS correlations suggest that higher quality films have higher values of the real impedance at ≈0.05 Hz and, hence, the quality of the films can be similarly ranked. Finally, phase angles at ≈10 Hz can be used to indicate the quality of the oxides: phase angles closer to −90° tend to be of higher quality. It can be seen in Table 4 that these mea-

Table 4
Rankings of oxide film quality.

Rank	Anodic polarization		EIS	
	Based on i_p (low i_p to high i_p)	Based on ϕ_c (high ϕ_c to low ϕ_c)	Based on Z_{real} at 0.05 Hz (high Z_{real} to low Z_{real})	Based on phase angle at 10 Hz (−90 to 0°)
(Highest quality)	3	7	7	10
	10	10	3	5
	7	3	10	3, 7, 4[b]
	5	5	5[b]	3, 7, 4[b]
	4	4	4[b]	3, 7, 4[b]
	1[a]	1[a]	6[a]	9[a]
	2[a]	6[a]	1[a]	6[a]
	6[a]	9[a]	8[a]	1[a]
	8[a]	8[a]	9[a]	2[a]
(Lowest quality)	9[a]	2[a]	2[a]	8[a]

[a] Solutions with $(SO_4)^{2-}$.
[b] Designates a tie.

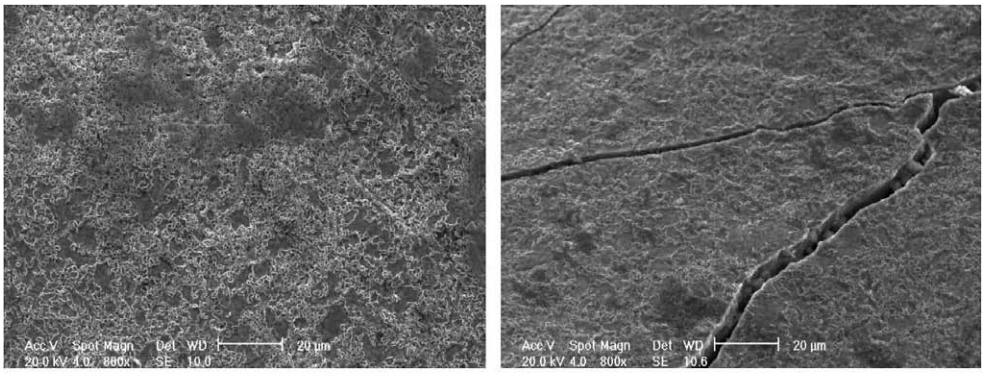

(a) $i_p = 0.83\ \mu A/cm^2$, $\phi_c = -214$ mV (b) $i_p = 15.95\ \mu A/cm^2$, $\phi_c = -563$ mV

Fig. 10. SEM images of rebar surface after immersion for 14 days in (a) Solution 10 and (b) Solution 9.

sures derived from both anodic polarization and EIS techniques provided very similar rankings for the oxide films These measures are not all independent, so it is not surprising that they lead to similar rankings; however, this shows that any of the measures can be used to provide an estimate of the quality of the protective oxide film. This could prove useful in practical situations where some measurements might be easier to make than others.

There were insufficient data to determine the functional dependencies of the passive film quality (as measured by the free-corrosion potential or the passive current density) on the concentrations of the ions, Ca^{2+}, Na^{+}, K^{+} and $(SO_4)^{2-}$, examined in this study. In addition, the passive current density was not correlated with pH (conductivity or oxygen content of the solutions), which suggested that pH might not be an important factor in determining film quality. However, pH does play a role by relating passive current density to free-corrosion potential through Eqs. (1) and (2), hence, passive current density and free-corrosion potential are strictly not independent indicators of passive film quality. This is a reminder that simple correlations can be misleading when the underlying mechanism is complex. More detailed studies are required to understand the effects on the quality of the passive film of pH, conductivity and oxygen content, and also the contributions of different amounts of various ions in the pore solution.

Finally, scanning electron microscope (SEM) images of as-received black steel rebar specimens exposed to solution 10 and solution 9 are presented in Fig. 10; the oxides formed in these solutions have low and high passive current densities, respectively. Fig. 10a shows that the rebar surface in solution 10 is uniform without cracks and pores. Fig. 10b shows solution 9 has cracks distributed over the surface of the rebar. In general, the SEM investigation revealed that relatively crack-free surfaces have higher corrosion potentials and lower passive current densities compared to those with more cracked surfaces. However, these results are preliminary and further microscopic investigations of the oxide film morphology and composition using other methods are required (e.g. transmission electron microscopy study of oxide cross sections).

4. Conclusions

The following conclusions can be drawn from the study presented in this paper:

- Ions commonly found in concrete pore solutions, such as Ca^{2+}, Na^{+}, K^{+} and $(SO_4)^{2-}$, can affect the passive oxide layer formed on common black reinforcing steel. Hence, even though concrete pore solutions are overwhelmingly composed of calcium hydroxide, the current results suggest the importance of these auxiliary ions during the formation of the oxide films. Further investigations are required to determine the functional details regarding how the quality of the passive film depends on different amounts of various ions in the pore solution, and on pH, conductivity and oxygen content.
- In particular, it has been observed by both anodic polarization and EIS that the presence of $(SO_4)^{2-}$ ions in the pore solution has a significant negative effect on the protective properties of passive oxide films.
- The experiments in this paper were designed to simulate in-service conditions of steel rebar in concrete; hence, no special surface preparation technique was used. Anodic polarization experiments that were carried out after 5, 8 and 14 days of immersion suggest that eight days are required for the oxides to stabilize. The stability of the tests after eight days of immersion indicates that reliable data can be obtained with as-received rebar, without special surface preparation, such as polishing.
- The analysis of anodic polarization curves obtained from different oxide films has led to the determination of the Tafel parameters for the oxygen reduction reaction on black steel rebar in synthetic concrete pore solutions ($\beta_c = -245 \pm 30$ mV/decade, $i_o = (1.4 \pm 0.9) \times 10^{-2}$ μA/cm^2). These values are consistent with previously reported cathodic Tafel slopes for oxygen reduction in alkaline solutions and in mortars. The method introduced in this study determines β_c from the passive current densities of a number of passive oxides and their corresponding free-corrosion potentials, which were used to map the cathodic activation polarization. This method is complementary to the standard approach, which relies on finding the linear region in a plot of the cathodic polarization vs. log current density; however, it does not have the same difficulties with defining the extent of the linear region.
- The protective properties of passive oxide films can be estimated with EIS at frequencies where there is a strong correlation between the free-corrosion potential and the measured impedances and phase angles: higher impedances at low frequencies (<1 Hz), and lower phase angles at mid frequencies (1–100 Hz) are good indicators of high quality protective oxides.

Acknowledgments

This research was supported by a grant from the Natural Sciences and Engineering Research Council (NSERC) of Canada along with technical and financial support of CANMET-MTL laboratories, through the Resource for Innovation of Engineered Materials program. Both contributions are gratefully acknowledged.

References

[1] Broomfield JP. Corrosion of steel in concrete: understanding, investigation and repair. London: E & FN Spon; 1997.
[2] Ahmad S. Reinforcement corrosion in concrete structures, its monitoring and service life prediction – a review. Cem Concr Compos 2003;25:459–71.
[3] Blanco G, Bautista A, Takenoutin H. EIS study of passivation of austenitic and duplex stainless steels reinforcement in simulated pore solution. Cem Concr Compos 2006;28:212–9.
[4] Monticelli C, Frignani A, Trabanelli G. Study on corrosion inhibitors for concrete application. Cem Concr Res 2000;30(4):635–42.
[5] Saremi M, Mahallati E. A study on chloride-induced depassivation of mild steel in simulated concrete pore solution. Cem Concr Res 2002;32(12):915–1921.
[6] Moragues A, Macias A, Andrade C. Equilibria of the chemical composition of the concrete pore solution. Part I: comparative study of synthetic and extracted solutions. Cem Concr Res 1987;17:173–82.
[7] Andersson K, Allard B, Bengtsson M, Magnusson B. Chemical composition of cement pore solutions. Cem Concr Res 1989;19:327–32.
[8] Page CL, Vennesland O. Pore solution compositions and chloride binding capacity of silica fume cement paste. Mater Struct 1983;16(1):19–25.
[9] Neville AM. Properties of concrete. 4th ed. Prentice Hall; 2005.
[10] Goni S, Andrade C. Synthetic concrete pore solution chemistry and rebar corrosion rate in the presence of chlorides. Cem Concr Res 1990;20(4):525–39.
[11] Macias A, Andrade C. Corrosion rate of galvanized steel in saturated solutions of $Ca(OH)_2$ in the pH range 12–13.8. Brit Corros J 1983;18(2):82–7.
[12] Poursaee A, Hansson CM. Reinforcing steel passivation in mortar and pore solution. Cem Concr Res 2007;37(7):1127–33.
[13] Mammoliti L, Hansson CM. Influence of cation on corrosion behavior of reinforcing steel in high-pH sulfate solutions. ACI Mater J 2005;102(4):279–85.
[14] Rondelli G, Lazzari L, Ormellese M, Rovoa R, Perez E. Study of carbon steel corrosion inhibition in alkaline solution by means of EIS. In: Marcus P, Maurice V, editors. Proceedings of the international conference on passivation of metals, and properties of thin oxide layers, Paris, 2006. p. 709.
[15] Montemor MF, Simoes AMP, Ferreira MGS. Analytical characterization of the passive film formed on steel in solutions simulating the concrete interstitial electrolyte. NACE Corros 1998;54(5):347–53.
[16] Gui J, Devine TM. The influence of sulfate ions on the surface enhanced Raman spectra of passive films formed on iron. Corros Sci 1994;36(3):441–62.
[17] Marcotte TD. Characterization of chloride-induced corrosion products that form in steel-reinforced cementitious materials. PhD thesis, Waterloo, University of Waterloo; 2001.
[18] Mahallati E, Saremi M. An assessment on the mill scale effects on the electrochemical characteristics of steel bars in concrete under DC-polarization. Cem Concr Res 2006;36(7):1324–9.

[19] Li L, Sagues AA. Chloride threshold of reinforcing steel in alkaline solutions – open-circuit immersion tests. NACE Corros 2001;57(1):19–28.
[20] ASTM G 5-94. Standard reference test method for making potentiostatic and potentiodynamic anodic polarization measurements. West Conshohocken (PA): Annual Book of ASTM Standards; 2007.
[21] Li L, Sagues AA. Chloride threshold of reinforcing steel in alkaline solutions – effect of specimen size. NACE Corros 2004;60(2):19–28.
[22] Raktoe BL, Hedayat A, Federer WT. Factorial design. John Wiley & Sons; 1981.
[23] Bird HEH, Pearson BR, Brook PA. The breakdown of passive films on iron. Corros Sci 1988;28(1):81–6.
[24] Li L, Sagues AA. Chloride threshold of reinforcing steel in alkaline solutions – cyclic polarization behaviour. NACE Corros 2002;58(4):305–16.
[25] Leckie HP. A contribution to the applicability of critical pitting potentials. J Electrochem Soc 1970;117(9):1152–4.
[26] Revie R, Uhlig HH. Corrosion and corrosion control. 4th ed. John Wiley & Sons; 2008.
[27] Conway E. Electrochemical data. New York, NY: Elsevier; 1952.
[28] Garcés P, Andrade C, Saez A, Alonso M. Corrosion of reinforcing steel in neutral and acid solutions simulating the electrolytic environments in the micropores of concrete in the propagation period. Corros Sci 2005;47(2):289–306.
[29] Jäggi S, Elsener B, Böhni H. Oxygen reduction on mild steel and stainless steel in alkaline solutions. In: Mietz J, Polder R, Elsener B, editors. Corrosion of reinforcement in concrete-corrosion mechanisms and corrosion protection, vol. 31. European Federation Publication EFC; 2000. p. 3–12.
[30] Brem M. Numerische Modellierung der Korrosion an Stahlbetonbauten. PhD thesis. ETH Zürich No. 15567, 2004.
[31] Mansfeld F. The polarization resistance technique for measuring corrosion currents. In: Fontana MG, Staehle RW, editors. Advances in corrosion science and technology, vol.6. New York: Plenum Press; 1976. p. 63.